

Review

# A Critical Review of the Material Characteristics of Additive Manufactured IN718 for High Temperature Application

Ching Kiat Yong \*, Gregory J. Gibbons and Geoff West

Warwick Manufacturing Group (WMG), University of Warwick, CV4 7AL Coventry, United Kingdom; [ching-kiat.yong@warwick.ac.uk](mailto:ching-kiat.yong@warwick.ac.uk) (C.K.); [G.J.Gibbons@warwick.ac.uk](mailto:G.J.Gibbons@warwick.ac.uk) (G.G.); [G.West@warwick.ac.uk](mailto:G.West@warwick.ac.uk) (G.W.)

**Abstract:** This paper reviews state of the art Additive Manufactured (AM) IN718 alloy intended for high temperature applications. AM processes have been around for decades and have gained traction in the past five years due to the huge economic benefit it brings to manufacturers. It is crucial for the scientific community to look into AM IN718 applicability in order to see a step-change in the production. Microstructural studies reveal that the grain structure plays a significant role in determining the fatigue lifespan of the material. Controlling IN718 respective phases such as the  $\gamma'$ ,  $\delta$  and Laves phase is seen to be crucial. Literature reviews have shown that the mechanical properties of AM IN718 were very close to its wrought counterpart when treated appropriately. Higher homogenization temperature and longer ageing were recommended to dissolve the damaging phases. Various surface enhancement techniques were examined to find out their compatibility to AM IN718 alloy that is intended for high temperature application. Laser shock peening (LSP) technology stands out due to the ability to impart low cold work which helps in containing the beneficial compressive residual stress it brings in high temperature fatigue environment.

**Keywords:** laser powder bed fusion; Inconel 718; high temperature; material characterisation; laser shock peening

---

## 1. Introduction

Additive Manufacturing (AM) is a promising technology for fabricating a wide range of structures and complex geometries from three dimensional (3D) model data. The process consists of depositing successive layers of material, one layer on top of another. AM was first developed by Chuck Hull in 1983, who established the process which was later known as stereolithography [1]. Designs are drawn using a computer-aided design (CAD) program which is then translated into model data. A 3D printer takes this data and slices it into several dimensional plans which instruct it where to deposit the layers of material. In 2015, the American Society of Testing and Materials (ASTM) issued a standard for AM technologies that consist of seven main processes [2], which established and defines the terms used in the field.

Alloys used for high temperature application are highly sought after in the aerospace and nuclear industry due to their high strength and stability at extreme temperatures. Alloys that operate at high temperature are critical for these industries as the efficiency of fuel conversion is closely related to the operating temperature. Generally, these alloys are nickel, iron or cobalt based. Its strength could sometimes become a weakness, as machining these alloys can be very difficult and expensive due to its natural tendency for work hardening. The shift to AM technology has allowed manufacturers to produce complex geometries such as lattice structures [3, 4], where traditional manufacturing such as casting or forging are a lot more time-consuming, or incapable of achieving these geometries. Researchers have made great efforts to understand the process-structure-property-performance relations to AM materials. Figure 1 illustrate a general material design chart with the intent to produce the most optimised mechanical properties suited for its intended application.

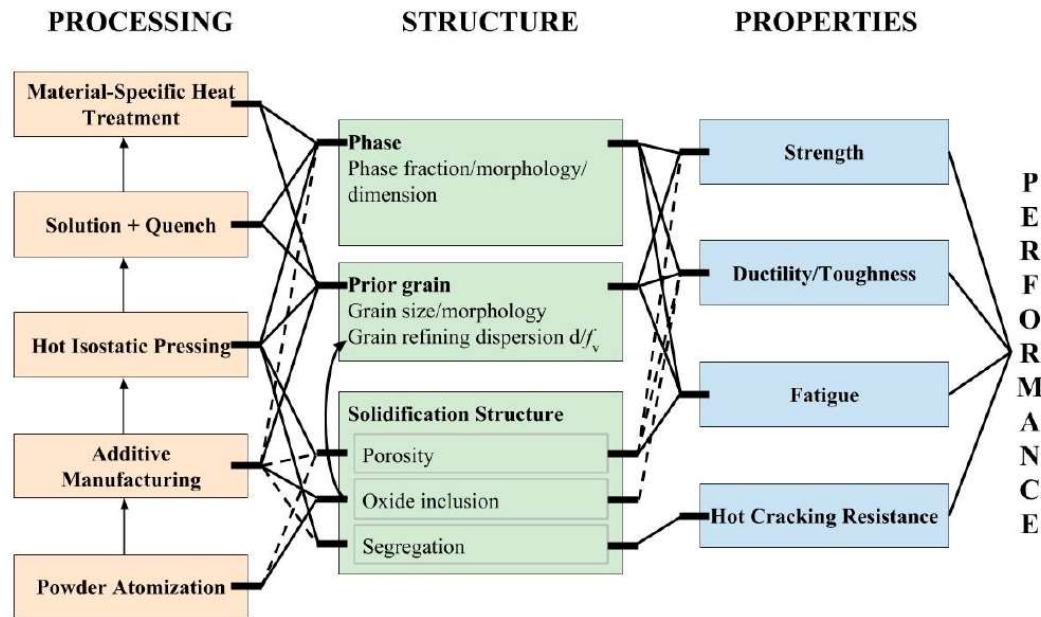


Figure 1. Material design chart that showcase the process-structure-properties-performance relationship for AM metal alloy, provided by [5]

This review paper aims to provide an overview of the AM of Inconel 718 (IN718), focusing on Powder Bed Fusion (PBF), which is one of the seven AM technologies. To the author's knowledge, a robust understanding of the fatigue response for AM IN718 in a high temperature environment remains elusive. The literature review covers the current research gap and challenges encountered in adopting AM IN718 for commercial use. Microstructural development and mechanical performances of AM IN718 are also discussed. Post-processing methods for AM IN718 are explored, as the scientific community sought out ways to push its usability for high temperature applications.

## 2. Additive Manufacturing

### 2.1 Benefits of the AM process

Reviews on the AM process have been covered thoroughly by many authors [6-11] and this section will focus on the seven technologies that were established by the ASTM community, and the benefits of each individual technology. Table 1 articulates the seven processes.

**Table 1.** Description of the AM technologies and benefits associated with it [6, 12-15]

Technologies	Description	Benefits
1. Powder Bed Fusion	Using a laser or electron beam to fuse thin layers of fine powders together, which are spread and closely packed on a platform. Subsequent layers of powders are applied on top of the previous layers until the final part is built	<ul style="list-style-type: none"> <li>• Fine resolution</li> <li>• High quality</li> </ul>
2. Direct Energy Deposition	A nozzle mounted on a multi axis arm, which deposits melted material onto the substrate	<ul style="list-style-type: none"> <li>• Suitable for reparation works</li> </ul>

		<ul style="list-style-type: none"> <li>• Good mechanical properties</li> </ul>
3. Material Jetting	Droplets of material are deposited from the nozzle onto the platform, where it solidifies and subsequent layers are built on it	<ul style="list-style-type: none"> <li>• Smooth surface finishing</li> <li>• Multi-material printing</li> </ul>
4. Binder Jetting	Utilize a binder that was deposited using an inkjet-print head to join materials in a powder bed	<ul style="list-style-type: none"> <li>• Parts can be made with a range of different colours</li> </ul>
5. Material Extrusion	Continuous filament of a polymer is heated and extruded onto the platform or on top of previous layers	<ul style="list-style-type: none"> <li>• Low cost</li> <li>• High speed</li> </ul>
6. VAT Photo-polymerization	A pre-deposited photopolymer in a vat is selectively cured by light	<ul style="list-style-type: none"> <li>• Fine resolution</li> <li>• High quality</li> </ul>
7. Sheet Lamination	Layer-by-layer cutting and lamination of sheets or ribbons of metal	<ul style="list-style-type: none"> <li>• Low cost</li> <li>• High speed</li> </ul>

## 2.2 Industrial Value

In the past 10 years, many companies have embraced AM technologies and are beginning to enjoy the real business benefits. In a report by Statista, the global 3D printer market size reached US\$7.3 billion in 2017 and the aerospace and defence sectors account for 17.8% of the market distribution in 2016 [16]. The global AM market is expected to see double digit growth into 2022 with market analysis projecting a growth of up to 35% per annum [17]. Recent developments such as cheaper metal powder [18] and the influx of new vendors [19] have significantly reduced the cost of the printers and AM has worked its way into a number of markets. The growing consensus of adopting AM into its production floor is attributed to several advantages over traditional manufacturing, as shown in Table 2.

**Table 2.** Advantages of AM over traditional manufacturing adapted from [20]

Areas of application	Advantages
1. Rapid Prototyping	<ul style="list-style-type: none"> <li>• Reduce time to market by accelerating prototyping</li> <li>• Reduce the cost involved in product development</li> <li>• Making companies more efficient and competitive at innovation</li> </ul>
2. Production of Spare Parts	<ul style="list-style-type: none"> <li>• Reduce repair times</li> <li>• Reduce labor cost</li> <li>• Avoid costly warehousing</li> </ul>

---

3. Small Volume Manufacturing	<ul style="list-style-type: none"> <li>• Small batches can be produced cost-efficiently</li> <li>• Eliminate the investment in tooling</li> </ul>
4. Customized Unique Items	<ul style="list-style-type: none"> <li>• Eliminate mass customization at low cost</li> <li>• Quick production of exact and customized replacement parts on site</li> <li>• Eliminate penalty for redesign</li> </ul>
5. Complex Work Pieces	<ul style="list-style-type: none"> <li>• Produce complex work pieces at low cost</li> </ul>
6. Machine Tool Manufacturing	<ul style="list-style-type: none"> <li>• Reduce labor cost</li> <li>• Avoid costly warehousing</li> <li>• Enables mass customization at low cost</li> </ul>
7. Rapid Manufacturing	<ul style="list-style-type: none"> <li>• Directly manufacturing finished components</li> <li>• Relatively inexpensive production of small number of parts</li> </ul>
8. Component Manufacturing	<ul style="list-style-type: none"> <li>• Enable customization at low cost</li> <li>• Improve quality</li> <li>• Shorten supply chain</li> <li>• Reduce the cost involved in development</li> <li>• Help eliminate excess parts</li> </ul>
9. On-site and On-demand Manufacturing of Replacement Parts	<ul style="list-style-type: none"> <li>• Eliminate storage and transportation cost</li> <li>• Reduce downtime</li> <li>• Shorten supply chain</li> <li>• Allow product lifecycle leverage</li> </ul>
10. Rapid Repair	<ul style="list-style-type: none"> <li>• Reduction in repair time</li> <li>• Opportunity to modify repaired components to the latest design</li> </ul>

---

A wide variety of materials can be utilized, but metals are generally popular due to their extensive use in industrial and consumer appliances. **Error! Reference source not found.** illustrates the activity map of selected aerospace companies, with many players focusing their research and development work on AM technology. General Electric (GE) leads the industry in terms of the both the volume and machine capacity, and have printed more than 100,000 parts by 2020. Rolls Royce, MTU Aero Engines, Pratt & Whitney and GKN Aerospace have established their own competencies centre to upskill their AM capabilities [17]. GE Aviation has been particularly successful in implementing AM technology into its product. In 2015, GE announced that the next LEAP engine will have nearly twenty 3D-printed fuel nozzles [21], simplifying parts by combining multiple components. Traditionally, the aerospace industry used advanced and costly materials like titanium and nickel alloys, which are difficult to manufacture and creates a large amount of waste. For example, Wilson et al [22] has shown that through the use of AM technology, his team was able to achieve a 45% carbon footprint improvement and a 36% savings in total energy over replacing it with an entirely new blade. In 2019, Rolls Royce produced its first AM low-pressure turbine for the Trent XWB-84 which is expected to result in a component weight reduction of up to 40% as well as generate significant cost savings for the company [23].

In a separate report made by Deloitte, it highlighted that AM technology has shown to bring the scrap rate to around 10-20% [24] while fabricating parts with intricate geometries such as internal cavities and lattice structures. Moreover, AM has the potential to lower overall cost as it is able to manufacture spare parts on demand, reducing maintenance time and the need for inventory management [25]. Boeing and Airbus typically sourced its 4 million spare parts around the globe, and airlines usually maintain an inventory of spares to avoid their planes from becoming grounded. AM technology is an enabler for these companies to embark on a supply chain transformation, making on-demand manufacturing possible. Combined with the outbreak of COVID19, companies are looking towards a “just in case” framework rather than “just in time” [26], specifically benefiting from the advanced production capability of AM processes.

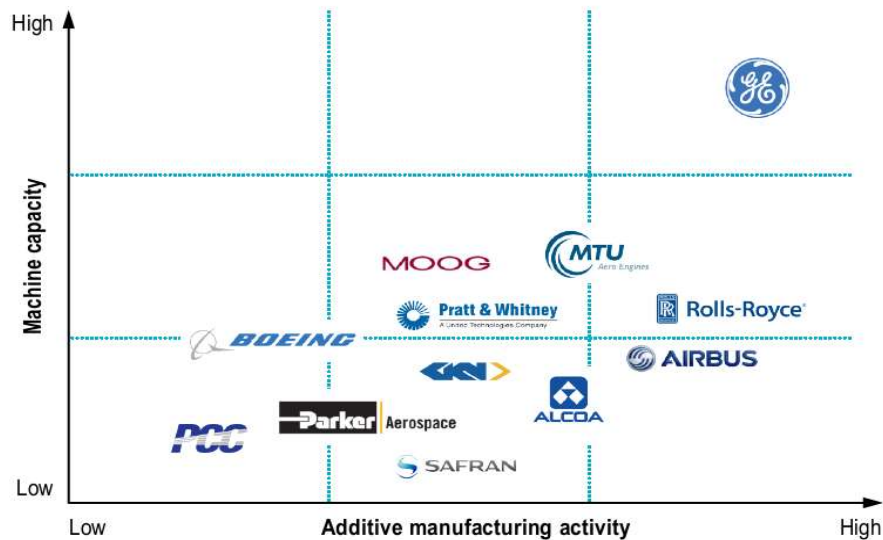


Figure 1. AM industry activity map of selected aerospace company taken from [17]

### 2.3 Types of Metal AM Process

Out of the seven main AM processes, powder bed fusion (PBF) and direct energy deposition (DED) are generally used to produce high quality metal parts. Lewandowski et al. [7] categorized these two mainstream processes into its respective energy source for fusion and the companies that have a specialization in them, as shown in Figure 2.

The DED process has a high degree of control and freedom as it can simultaneously feed multiple types of powders through its nozzle, as shown in Figure 3a. By adjusting the feed rate, it is feasible to achieve desirable microstructural features and chemical composition which is favourable for building functionally graded materials [27] or structural metal components [13]. Apart from manufacturing near net shape components, DED is suitable for repairing high value parts with little wastage [28-30]. This capability enables manufacturers to remanufacture turbine blades with cracks and voids which is economically viable and helps in design enhancements at the time of restoration [22]. Consequently, remanufacturing using accurate AM processes will enable industries to save energy and material, and contribute towards sustainable design and manufacturing. Despite its benefits, DED faces several challenges with its quality and efficiency. Resolutions are generally very low and parts have a rough surface finish that may need post-processing such as by machining to obtain tight tolerances [10].

PBF has a unique position because of its potential to manufacture metal components in a range of alloys, at high resolution and accuracy, which has broadened the application to various industries. The process consists of depositing thin layers of fine powder on a platform which is then fused together with a laser or electron beam, as shown in Figure 3b. Many metallic materials such as

stainless and tool steels, aluminium alloys, titanium and its alloys, and nickel-based alloys can be manufactured by this process.

The main differences between DED and PBF is the way that that powder is fed. In PBF, metal powders are uniformly spread by a rake or roller, while in DED, powders are blown out from the nozzle. The high precision of PBF allows for the optimisation of component design and manufacturing cost. For example, GE aviation have been using metal PBF machines to manufacture its fuel nozzles and next-generation materials, including heat-resistant ceramic matrix composites (CMCs) and carbon fibre blades. The fuel nozzles were five times more durable than the previous model and reduced the number of required parts from twenty-five to just five [21].

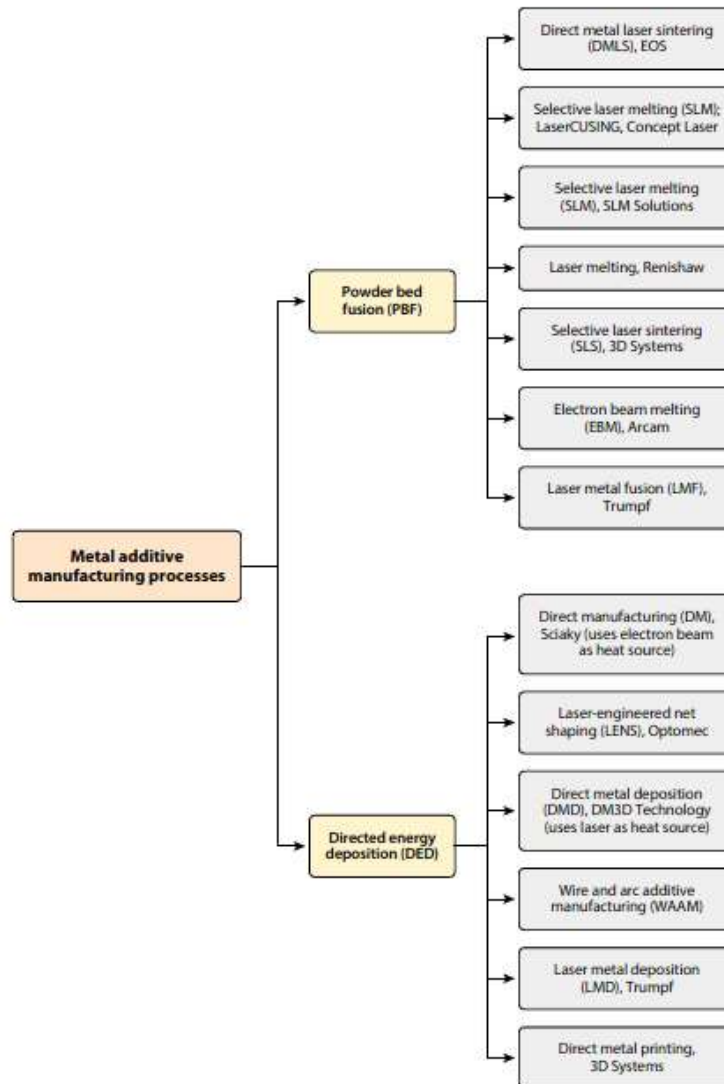


Figure 2. Various AM processes adapted from [7]

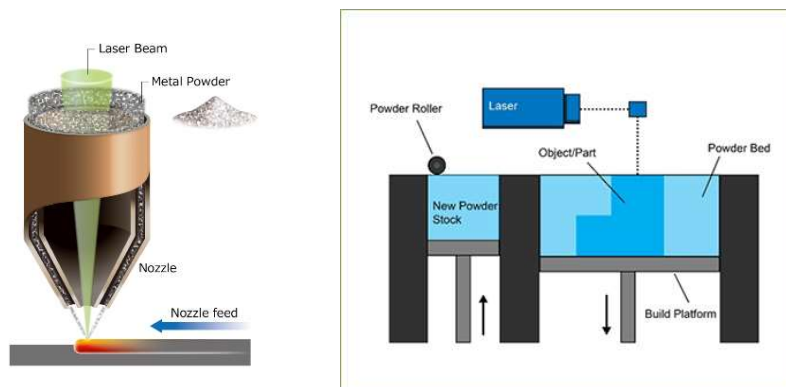


Figure 3. Schematic diagram of (a) DED [31] and (b) PBF adapted from [32]

Another successful case study came from Arconic, where the company managed to install its 3D printed titanium brackets on the airframe of an Airbus A350 XWB commercial plane, which helps to lower the wastage of raw materials by 80% as compared to manufacturing it conventionally [33]. Some of the common materials which have been processed by PBF are listed in **Error! Reference source not found.**

Table 3. Common alloys processed by PBF

Alloy	Examples	Reference
Titanium	Ti-6Al-4V, Ti-6.5Al-1Mo-1V-2Zr, Ti-6.5Al-3.5Mo-1.5Zr-0.3Si, Ti-5Al-4Mo-2Zr-2Sn-4Cr, Ti-3Al-10V-2Fe	[34-46]
Intermetallics	NiTi	[47-50]
Steel	316L, 17-4PH, AISI 420	[51-56]
Nickel	IN718, IN625, C263, Hastelloy X, K418	[57-93]
Aluminium	Al-Si10-Mg, Al-Si12-Mg, 6061	[41, 94, 95]

IN718 is the most commonly used nickel-based alloy in the aerospace industry due to its superior mechanical properties at elevated temperatures and has been widely used in the turbine section of the aeroengine [96-98]. It has the ability to withstand loading at an operating temperature close to its melting point of 1336°C [99]. It has a high phase stability of face-centered-cubic (FCC) nickel matrix and the capability to be strengthened by other alloys such as chromium and/or aluminium [100]. The microstructure of IN718 is referred to by  $\gamma$  (gamma), a continuous matrix phase where cobalt and chromium prefers to reside;  $\gamma'$  (gamma prime), an intermetallic phase based on  $\text{Ni}_3(\text{Al,Ti})$  with a  $L_{12}$  crystal structure;  $\gamma''$  (gamma double prime), a metastable phase that is the primary strengthening precipitate with a body-centered tetragonal (BCT) ordered compound with a  $D0_{22}$  crystal structure;  $\delta$  (delta), an equilibrium phase with an orthorhombic  $D0_a$  structure; Laves phase with an embrittling TCP phase; carbides and borides that prefer to reside on the grain boundaries [12, 101, 102]. However, the usage of PBF IN718 in the aeroengine has been an obstacle owing to the presence of undesirable phases [103] and its unconventional microstructure [73, 103, 104]. Efforts have been made to limit these defects through the use of heat treatment [61, 103] and hot isostatic pressing (HIP-ing) [67], but the results have been mixed and no significant improvements have been made on PBF IN718.

### 3. Microstructure of AM IN718

#### 3.1 Grain Structure

In this review, grain structure constitutes both grain size and grain texture of the material. Unlike its wrought counterpart, AM IN718 display a mixture of columnar and equiaxed grains when no additional treatment is applied. This is due to its uneven cooling rate as the material is being built up layer by layer. Factors such as heat flux and thermal gradients greatly affect the growth of the grains, which are not discussed in this paper. Interested readers could look at the references given here [86, 105-107]. Ahmad et al. [103] showed that AM IN718 has columnar grain growing parallel to the building direction. A magnified image using optical microscopy of the microstructure of AM IN718 without any additional treatment is shown in Figure 4.

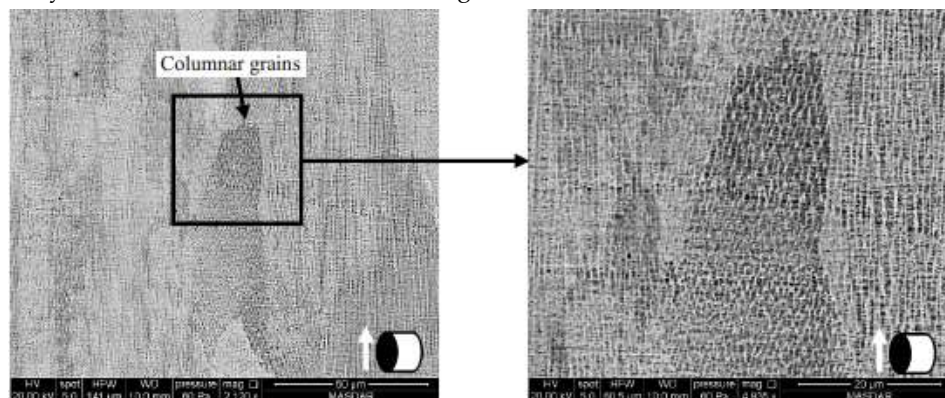


Figure 4. An optical image showing the columnar grains of AM IN718, taken from [103]

Gribbin et al. [108] took one step further and utilized electron backscatter diffraction (EBSD) to investigate the crystallographic structure of the material. As-built AM IN718 exhibits elongated grain structure with a moderate  $\langle 100 \rangle$  fibre texture formed along the build direction, as shown in Figure 5. Fatigue strength of the wrought alloy outperforms the AM alloy at room temperature, suggesting the grain texture is likely the main competing microstructural feature affecting the fatigue performances at room temperature. The microstructural study findings were comparable to other studies as well [63, 73, 79, 109], although fatigue life is known to be generally dominated by surface characteristic such as surface roughness [42, 110-112] and porosity [72, 113], and thus the conclusion made by Gribbin et al. might be incomplete and further investigation has to be made. The fatigue response of the as-built AM material had a similar response to the wrought material at elevated temperature of 500 °C. Both materials had a fatigue limit of approximately 600 MPa [108] despite AM IN718's inherent weakness of high content of  $\delta$  precipitates, which is known to deteriorate the fatigue behaviour at high temperature. This suggests that the difference in microstructural features is not pronounced in high temperature environments as compared to the room temperature condition.

Another interesting finding on wrought IN718 in elevated temperature has [114] shown that the coarse-grain alloy has a fatigue strength significantly lower than fine-grain alloy when it is beyond  $10^5$  cycles. It is likely that in order to maximize AM IN718 capability in high temperature applications, controlling the grain size of the alloy will be vital, and any grain size refinement technique for AM metal alloys will be welcome.

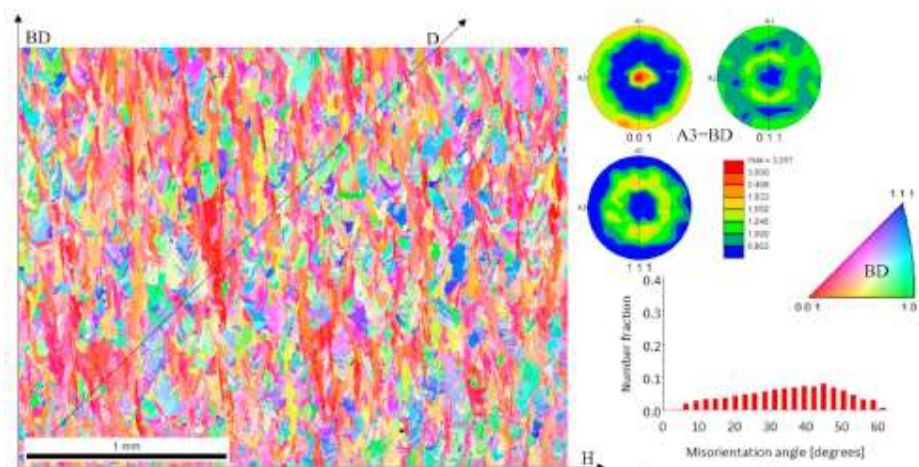


Figure 5. EBSD map and the pole figures showing the crystallographic texture of as-built AM IN718, taken from [108]

### 3.2 Effects of $\delta$ phases

IN718 is a precipitation-strengthened nickel-based superalloy with  $\gamma''$  as the main phase contributing to its excellent high temperature strength [115]. However, the metastable  $\gamma''$  phase easily transforms to a stable  $\delta$  phase under certain thermal conditions, decreasing the volume fraction of  $\gamma''$ , which indirectly affects the mechanical properties of the alloy [116]. It is generally undesirable as it is known to decrease the fracture toughness and ductility of the material [117, 118].  $\delta$  precipitates usually formed during the heat treatment process or during service, mainly resides at the grain boundaries [119]. However, there are cases where  $\delta$  precipitates have shown to display beneficial effects such as grain stabilization [120] and increasing stress rupture resistance [121]. An et al. [122] investigated the role of the  $\delta$  phase for fatigue crack propagation behaviour in wrought IN718 and showed that the growth rate increases with increasing  $\delta$  phase volume fractions. There were both long needle-like and granular shaped  $\delta$  precipitates present in the alloy which have very different effects on the fatigue crack growth. When  $\gamma''$  transforms into long needle-like  $\delta$  precipitates, precipitates free zone formed around the  $\delta$  phase, inhibiting micro cracks that are detrimental to the fatigue performance of the alloy. While the granular shaped  $\delta$  precipitates, with low length-diameter ratio, act as a pin between the grain boundaries, increasing the strength of the alloy.

AM IN718 usually has a slight variation on the volume fraction of its respective phases. In Gribbin's study, the  $\delta$  phase content in wrought IN718 was  $1.6\% \pm 0.5\%$  while the as-built AM IN718 contained  $3.8\% \pm 0.4\%$  [108], which is rather unusual for the IN718 alloy. The increase of the  $\delta$  phase content could be due to the heat treatment used to solution treat the alloy, leaving the precipitates undissolved. Yang et al. [123] compared the microstructure and mechanical performances of PBF-fabricated IN 718 alloy in various heat treatment conditions. The results show that the morphology and distributions of the  $\delta$  phase are key factors determining their high temperature performance. Too much  $\delta$  phase along the grain boundaries could cause dislocation to pile up [79], causing local stress concentrations and premature failure. Whereas the lack of the  $\delta$  phase will reduce the strength of the alloy at elevated temperature as it will have limited influence of the pinning effect on grain boundaries.

Formation of intragranular  $\delta$  precipitates was also observed in AM IN718, which is a common observation for IN718 alloy when the parameters of the heat treatment are not optimized [116]. Presence of high concentrations of niobium in the feedstock [108], combined with the inconsistent heat flux caused by heating and melting of the powder, is the reason why intragranular  $\delta$  precipitates are formed. Maximizing the volume fraction of intergranular  $\delta$  precipitates gives the alloy better ductility while a high amount of intragranular  $\delta$  precipitates hardens the material [116]. The ratio

between intragranular and intergranular precipitates could be a critical parameter in optimizing the mechanical properties at elevated temperature of AM IN718 based on the past studies.

### 3.3 Effects of Laves phases

Niobium is one of the elements present in IN718 and it is highly prone to segregation and tends to form some undesirable phases such as the  $\delta$  and the Laves phases, which is known for degrading tensile ductility, fatigue and creep rupture properties [124-126]. High concentration of niobium has been reported by other researchers which catalyse the formation of Laves phase, depleting the strengthening  $Y'$  phase. The Laves phase provides crack initiation and propagation sites during the melting of the metal powder [125] and is a general observation when IN718 alloy undergoes a process in a high temperature environment [127] such as heat treatment [61, 128, 129] or during the powder deposition of the AM process [66, 109, 130].

The presence of Laves phase generally deteriorates the ductility, ultimate tensile strength [131] and fatigue life of IN718 alloy [132]. Sui et al. [71] reported that AM IN718 alloy outperforms its wrought counterpart at low stress amplitude due to the role that the Laves phase played during the crack propagation stage. Whereas at high stress amplitude, almost all the Laves phase splintered into small fragments that caused microscopic holes or cracks to form. The S-N diagram developed by Sui et al. is shown in Figure 7. The existence of a micron-scaled Laves phase led to local stress concentrations more easily than the wrought alloy, causing it to break up at high stress amplitude. A schematic diagram on the fragmentation of the Laves phase is shown in Figure 8.

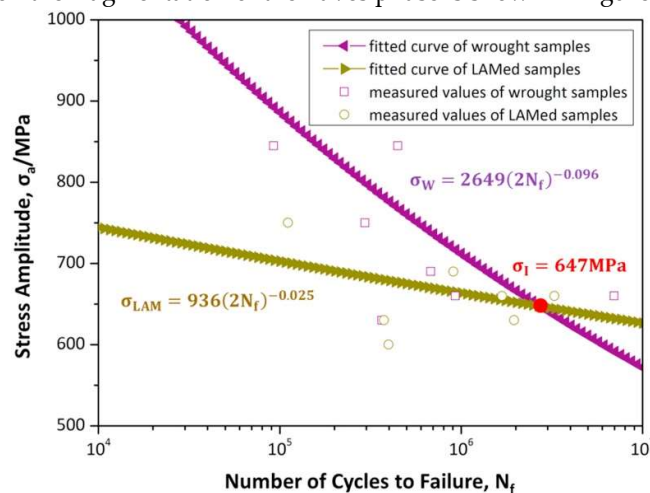


Figure 7. High cycle properties of wrought (in purple) and AM (in green) IN718 alloy, taken from [71]

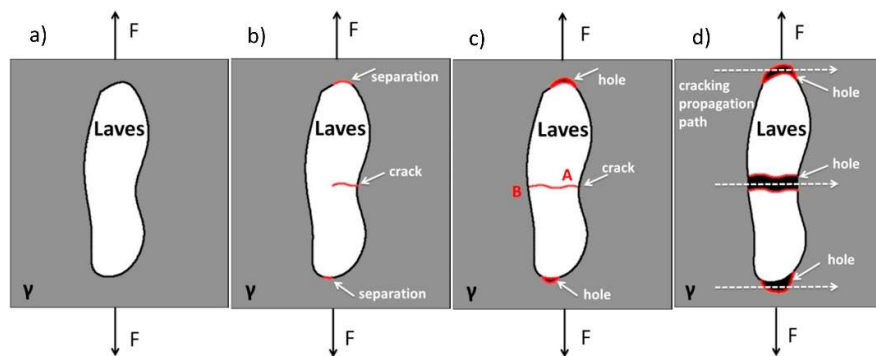


Figure 8. Schematic diagram showing the breaking up of Laves phase at high amplitude [71]

To the best of the author's knowledge, there have been no studies made on the effect of the Laves phase on the properties affecting the fatigue life of AM IN718 at high temperature. It is generally

regarded as a “parasitic” phase that consumes the available niobium content. Studies have shown that by either increasing the homogenization temperature or time [115, 133] could lower the volume fraction of the Laves phase. Laves and carbide are generally dissolved resulting in releasing a considerable amount of niobium back to the  $\gamma'$  matrix [129]. With that knowledge in mind, it is advisable to formulate new heat treatment standards cater for AM IN718 alloy that is entirely different from the AMS standards that the industry currently use.

#### 4. Mechanical Properties of PBF IN718 alloy

Table 4 present the previous work on the mechanical testing for PBF IN718 alloy. Most of the test data are rather similar with slight differences due to either the geometry of the test piece or the direction of the test piece when it's being tested. Generally, a post-processing step such as heat treatment or HIP-ing gives a better tensile strength but with a slight dip in its ductility. There were some instances where the tensile properties were superior to the wrought ones, giving the manufacturer extra confidence in employing AM IN718 on its production line. Researchers such as Strößner et al. [104] and Gallmeyer et al. [134] have attempted to optimize the heat treatment process by increasing its homogenization or ageing temperature and thereby controlling the growth of the  $\gamma'$  phase, and minimizing the impact of either the  $\delta$  or Laves phases, resulting in an increase in the strength and hardness of the material.

Data about the fatigue strength of PBF IN718 alloy was limited as it usually costs a significant amount of resources to be developed. Fatigue test are typically conducted on servo hydraulic test machines which are capable of applying large amplitude cycles over a long period of time [135]. It is heavily used in high-value industries such as the aerospace and biomedical sectors where safety standards are much stringent than in other sectors. For AM IN718 alloy to be used in a safety-critical application, it is vital to understand the process-structure-property relationship, and the availability of fatigue data gives extra confidence for manufacturers to utilize this technology. At the same time, several problems such as weak grain texture and detrimental residual stress [35, 108, 136] have to be dealt with in order to widen the adoption of AM IN718 alloy. This drives a need to introduce novel post-processing methods to improve the quality of AM products, which will be discussed in the next section.

Table 4 Summary of mechanical properties of PBF IN718 alloy

Condition	UTS/MPa	YS/MPa	El/%	Stress ratio	Loading frequency / Hz	Cycles to failure	Reference
As-built	1110 ± 11	711 ± 14	24.5 ± 1.1	-	-	-	[77]
	1167 ± 10	858 ± 12	21.5 ± 1.3	-	-	-	[77]
	845	580	21.5 ± 1.3	-	-	-	[77]
	1010 ± 10	737 ± 4	20	-	-	-	[77]
	997.8	800	20.6 ± 2.1	-	-	-	[77]
	1335	760	21.3	-	-	-	[134]
	1142.5 ± 5.5	898 ± 9	22.55 ± 3.35	-	-	-	[66]
As-built, heat treated	1451	1174	13.5	-	-	-	[62]
	1370 ± 25	-	22.2 ± 2	-	-	-	[70]
	1221	1007	16.0	-	-	-	[75]
	-	-	-	0	20	2x10 <sup>6</sup> (run out)	[137]
	1085 ± 11	816 ± 24	19.1 ± 0.7	-	-	-	[104]
	1010 ± 10	737 ± 4	20.6 ± 2.1	-	-	-	[104]
1417 ± 4	1222 ± 26	15.9 ± 1.0	-	-	-	[104]	

	1387 ± 12	1186 ± 23	17.4 ± 0.4	-	-	-	[104]
	1325	620	28.6				SA980 [134]
	1530	1135	10.6				SHT-1 [134]
	1560	1240	11.6				SHT-2 [134]
	1500	1120	14.5				DA620 [134]
	1580	1300	9.6				DA720 [134]
	1640	1245	16.6				SA1020 + A720 [134]
	1319 ± 39	1131.5 ± 29.5	16 ± 6				[66]
As-built, HIP-ed, heat treated	1200	890	28	-	-	-	[102]
	1384 ± 8	1123 ± 13	21.5 ± 3.5	-	-	-	[138]
Wrought	1241	1034	10	-	-	-	AMS 5662 [139]
	1610	1160	13.5				[134]
As-cast	802	758	5	-	-	-	AMS 5383 [139]

### 5. Suitability of Surface Enhancement Process

Surface treatments, such as shot-peening [140], deep-rolling [141] and laser shock peening (LSP) [142] are commonly used to increase the usability of AM materials. For high temperature applications, LSP has additional advantages over other surface treatments due to its ability to impart deep compressive residual stresses [143], lower cold work on the surface [144] and the ability for grain refinements [145, 146]. Inherently, the LSP process introduces high strain rates up to  $10^6 \text{ s}^{-1}$  which generate beneficial dislocations near the surface layer [147-149].

Table 5 Comparison of shot peening and LSP

	Strain rate ( $\text{s}^{-1}$ )	Cold work (%)	Depth (mm)	Typical roughness Ra ( $\mu\text{m}$ )
Shot peen (X20 Steel)	$10^3 - 10^4$	15 – 50	0.2	4.52
LSP (X20 Steel)	$10^6 - 10^7$	5 – 7	1.2	0.98
Shot peen (Ti-6Al-4V)	-	75	Surface	-
LSP (Ti-6Al-4V)	-	1 – 2	Surface	-
Shot peen (IN718)	-	30	Surface	-
LSP (IN718)	-	3 – 6	Surface	-

Table 5 compares the effects of shot peening and LSP on strain rate, cold work, depth of influence and the typical roughness of wrought X20 steel. LSP brings about a significant lower cold work as compared to shot peening. Lower amount of cold work was also observed in Ti-6Al-4V titanium alloy [150] and IN718 nickel coupons where the cold work was approximately 2% [144]. The difference in cold work between the X20 Steel and IN718 alloy is mainly due to the material's deformation capability. Although it is beyond the scope of this work to discuss shot peening, it is useful to bring it up as a comparison to LSP as it is a widely adapted technique in the industry. Shot peening involves

multiple steel or ceramic shots projected at a high velocity through a nozzle, striking the surface with force sufficient to create plastic deformation. Due to the continuous shots, most of the energy is expended in inducing plastic deformation, resulting in a highly cold worked surface layer [150]. On the other hand, LSP produces remarkably low cold work on the surface at room temperature [151], as shown in Figure 9. The cold work produced by shot peening comes close to 0% after a depth of  $10 \times 10^{-3}$  inch, dropping from the initial 30%. This begs the question why LSP is able to drive similar or higher compressive residual stresses and yet produce a lower amount of cold work on the surface. A high degree of cold work has been found to relax rapidly at high temperature [150-152] which is detrimental for high temperature application in the nuclear and aerospace industry. LSP might be in a more advantageous position than shot peening if it's able to withstand thermal stress relaxation in these industries. More investigation has to be done to find out the process-structure-property-performance relationship, utilising advanced material characterisation method such as EBSD or Transmission Electron Microscopy (TEM).

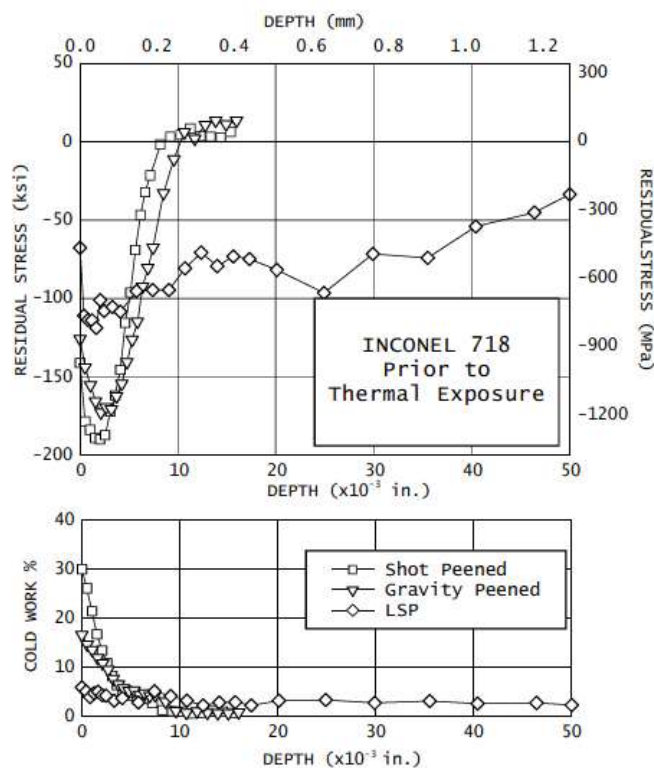


Figure 9. Taken from [150], residual stress distribution and cold work developed by in IN718 coupons using various surface enhancement process

There are other interesting research where LSP is being used as a post-processing step for AM metal components such as aluminium [153], stainless steel [154] and titanium alloy [142]. Kalentics et al. [154, 155] have proposed using LSP to tailor the residual stresses of stainless steel samples by moving the baseplate back and forth from a printing machine to a LSP station. He has dubbed it as 3D LSP, an ex-situ LSP and AM process which has shown to increase both magnitude and depth of compressive residual stress. The depth of compressive residual stress could reach up to 1 mm for an AM 316L stainless steel component subjected to the 3D LSP principle, as shown in Figure 11.

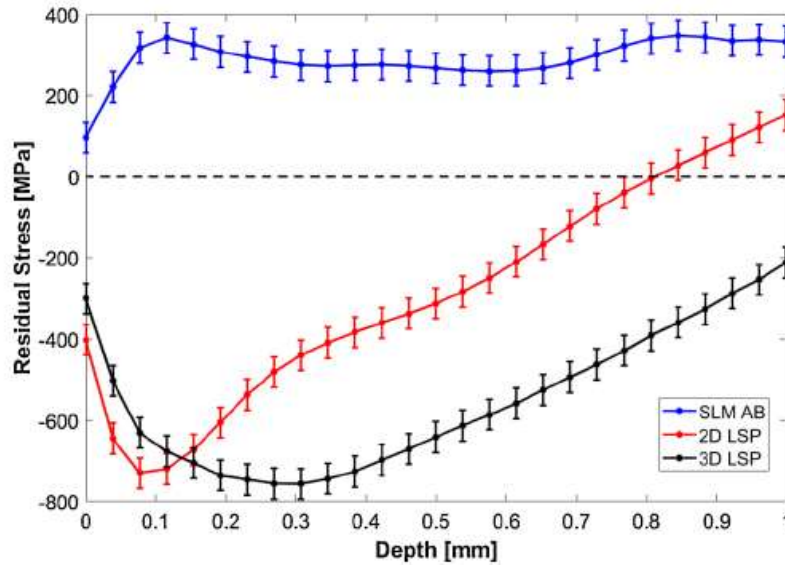


Figure 11. Taken from [154], residual stress curve measured for 316L Stainless Steel for as-built (AB), LSP after AM (2D LSP) and ex-situ LSP on AM (3D LSP)

## 6. Conclusion

The current priority of aeroengine manufacturers is to investigate the applicability of AM components in their manufacturing process as it offers significant processing flexibility and potential cost reduction. IN718 is one of those metal alloys that is suitable for the AM process route as it allows manufacturers to process it in an easy and straightforward way that ensures that the material properties are still well preserved. With layer-wise building of components, the process produces up to about 5% waste, reducing the raw material wastage significantly as compared to manufacturing it conventionally for aeroengine components.

Inherently, as-built AM products give a mixture of columnar and equiaxed grains which directly impacts the mechanical properties of the material at room temperature. At high temperature usage, its effect is not as prominent, and grain size will be the crucial factor in determining its fatigue life. Further research should be performed to identify the effects of the various phases present in the alloy that affects the usability of the material. It should be possible to control the growth of  $\gamma'$ ,  $\delta$  and Laves to maximize the properties of AM IN718 alloy which is suited for its intended application.

Numerous heat treatment procedures have been attempted by the scientific community to match its tensile strength with the wrought alloy. Higher homogenization temperature and longer ageing time is usually employed to reduce the presence of harmful phases such as the  $\delta$  and Laves phases. Such knowledge is important for developing beneficial microstructures and material properties for its intended application.

Analysis obtained from the literature suggest that the mechanical properties of PBF IN718 alloy were very similar to its wrought counterpart. However, there were insufficient experimental data to showcase the fatigue lifespan of AM IN718 alloy due to the complexity and high cost of the experiments.

Surface enhancement techniques were explored in this study as it could assist AM IN718 alloy to perform better in high temperature applications. LSP has the potential to be a suitable technique as it could induce lower amount of cold work which is beneficial in a high temperature environment.

**Author Contributions:** Conceptualisation, literature review and writing of the manuscript were done by C.K. Supervision and review of the manuscript performed by G.G and G.W. All authors have read and agreed to the published version of the manuscript

**Funding:** This research was funded by Agency for Science, Technology and Research (A\*STAR) Singapore and Warwick Manufacturing Group (WGM), University of Warwick.

**Acknowledgments:** This research is part of the EngD project that is sponsored by A\*STAR and the authors are thankful for the funding.

**Conflicts of Interest:** The authors declare no conflicts of interest.

## References

1. Systems, D. *Our Story*. 2019; Available from: <https://uk.3dsystems.com/our-story>.
2. ASTM *Standard Terminology for Additive Manufacturing – General Principles – Terminology*. 2015. DOI: 10.1520/ISOASTM52900-15.
3. Wen, Y., S. Xun, M. Haoye, S. Baichuan, C. Peng, L. Xuejian, Z. Kaihong, Y. Xuan, P. Jiang, and L. Shibi, *3D printed porous ceramic scaffolds for bone tissue engineering: a review*. *Biomater Sci*, 2017. **5**(9): p. 1690-1698.
4. Maconachie, T., M. Leary, B. Lozanovski, X. Zhang, M. Qian, O. Faruque, and M. Brandt, *SLM lattice structures: Properties, performance, applications and challenges*. *Materials & Design*, 2019. **183**: p. 108137.
5. Yan, F., W. Xiong, and E. Faierson, *Grain Structure Control of Additively Manufactured Metallic Materials*. *Materials*, 2017. **10**(11).
6. Ngo, T.D., A. Kashani, G. Imbalzano, K.T.Q. Nguyen, and D. Hui, *Additive manufacturing (3D printing): A review of materials, methods, applications and challenges*. *Composites Part B: Engineering*, 2018. **143**: p. 172-196.
7. Lewandowski, J.J. and M. Seifi, *Metal Additive Manufacturing: A Review of Mechanical Properties*. *Annual Review of Materials Research*, 2016. **46**(1): p. 151-186.
8. Zhang, Y., L. Wu, X. Guo, S. Kane, Y. Deng, Y.-G. Jung, J.-H. Lee, and J. Zhang, *Additive Manufacturing of Metallic Materials: A Review*. *Journal of Materials Engineering and Performance*, 2018. **27**(1): p. 1-13.
9. Wong, K.V. and A. Hernandez, *A Review of Additive Manufacturing*. *ISRN Mechanical Engineering*, 2012. **2012**: p. 208760.
10. Saboori, A., D. Gallo, S. Biamino, P. Fino, and M. Lombardi, *An Overview of Additive Manufacturing of Titanium Components by Directed Energy Deposition: Microstructure and Mechanical Properties*. *Applied Sciences*, 2017. **7**(9).
11. Frazier, W.E., *Metal Additive Manufacturing: A Review*. *Journal of Materials Engineering and Performance*, 2014. **23**(6): p. 1917-1928.
12. Gibson, I., D.W. Rosen, and B. Stucker, *Additive Manufacturing Technologies*. 2010.
13. Graf, B., A. Gumenyuk, and M. Rethmeier, *Laser Metal Deposition as Repair Technology for Stainless Steel and Titanium Alloys*. *Physics Procedia*, 2012. **39**: p. 376-381.
14. University, L. *Material Jetting*. About Additive Manufacturing; Available from: <https://www.lboro.ac.uk/research/amrg/about/the7categoriesofadditivemanufacturing/materialjetting/>.
15. University, L. *Binder Jetting*. About Additive Manufacturing; Available from: <https://www.lboro.ac.uk/research/amrg/about/the7categoriesofadditivemanufacturing/binderjetting/>.
16. Statista, *3D printing market distribution worldwide in 2016, by use case*. 2016.
17. Berger, R., *Additive Manufacturing in Aerospace and Defense*. 2017.
18. Medina, F., *Reducing metal alloy powder costs for use in powder bed fusion additive manufacturing: improving the economics for production*, in *Materials Science and Engineering*. 2013, University of Texas: El Paso.
19. Manufacturing, A. *The Additive Manufacturing Industry Landscape 2020: 240 Companies Driving Digital Manufacturing*. 2020 [cited 2020; Available from: <https://amfg.ai/2020/05/26/the-additive-manufacturing-industry-landscape-2020-231-companies-driving-digital-manufacturing/>].
20. Attaran, M., *The rise of 3-D printing: The advantages of additive manufacturing over traditional manufacturing*. *Business Horizons*, 2017. **60**(5): p. 677-688.
21. Kellner, T. *Fit to Print: New Plant Will Assemble World's First Passenger Jet Engine With 3D Printed Fuel Nozzles*, *Next-Gen Materials*. 2014; Available from: <https://www.ge.com/reports/post/80701924024/fit-to-print/>.

22. Wilson, J.M., C. Piya, Y.C. Shin, F. Zhao, and K. Ramani, *Remanufacturing of turbine blades by laser direct deposition with its energy and environmental impact analysis*. Journal of Cleaner Production, 2014. **80**: p. 170-178.
23. 2019 Annual Report. 2020, Rolls Royce plc.
24. Cotteleer, M., J. Holdowsky, M. Mahto, and J. Coykendall. *3D opportunity for aerospace and defense : Additive manufacturing takes flight*. 2014; Available from: <https://www2.deloitte.com/insights/us/en/focus/3d-opportunity/additive-manufacturing-3d-opportunity-in-aerospace.html>.
25. Khajavi, S.H., J. Partanen, and J. Holmström, *Additive manufacturing in the spare parts supply chain*. Computers in Industry, 2014. **65**(1): p. 50-63.
26. Board, E., *Companies should shift from 'just in time' to 'just in case'*, in *Financial Times*. 2020.
27. Wilson, J.M. and Y.C. Shin, *Microstructure and wear properties of laser-deposited functionally graded Inconel 690 reinforced with TiC*. Surface and Coatings Technology, 2012. **207**: p. 517-522.
28. Zhong, C., J. Kittel, A. Gasser, and J.H. Schleifenbaum, *Study of nickel-based super-alloys Inconel 718 and Inconel 625 in high-deposition-rate laser metal deposition*. Optics & Laser Technology, 2019. **109**: p. 352-360.
29. Sun, G.F., X.T. Shen, Z.D. Wang, M.J. Zhan, S. Yao, R. Zhou, and Z.H. Ni, *Laser metal deposition as repair technology for 316L stainless steel: Influence of feeding powder compositions on microstructure and mechanical properties*. Optics & Laser Technology, 2019. **109**: p. 71-83.
30. Kumar, L.J. and P.C.G.K. Nair, *Laser metal deposition repair applications for Inconel 718 alloy*. 2016.
31. Mitsubishi Heavy Industries Machine Tool. *Directed Energy Deposition AM System - LAMDA series*. [cited 2020; Available from: <https://www.mhi-machinetool.com/en/products/detail/lamda.html>].
32. University, L. *The 7 Categories of Additive Manufacturing*. Available from: <https://www.lboro.ac.uk/research/amrg/about/the7categoriesofadditivemanufacturing/>.
33. Molitch-Hou, M. *Arconic Talks Installing 3D-Printed Bracket on Series Production Commercial Airbus Airframe*. 2017; Available from: <https://www.engineering.com/3DPrinting/3DPrintingArticles/ArticleID/15709/Arconic-Talks-Installing-3D-Printed-Bracket-on-Series-Production-Commercial-Airbus-Airframe.aspx>.
34. Zhu, Y.-Y., H.-B. Tang, Z. Li, C. Xu, and B. He, *Solidification behavior and grain morphology of laser additive manufacturing titanium alloys*. Journal of Alloys and Compounds, 2019. **777**: p. 712-716.
35. Benedetti, M., V. Fontanari, M. Bandini, F. Zanini, and S. Carmignato, *Low- and high-cycle fatigue resistance of Ti-6Al-4V ELI additively manufactured via selective laser melting: Mean stress and defect sensitivity*. International Journal of Fatigue, 2018. **107**: p. 96-109.
36. Chern, A.H., P. Nandwana, T. Yuan, M.M. Kirka, R.R. Dehoff, P.K. Liaw, and C.E. Duty, *A review on the fatigue behavior of Ti-6Al-4V fabricated by electron beam melting additive manufacturing*. International Journal of Fatigue, 2019. **119**: p. 173-184.
37. Fatemi, A., R. Molaei, S. Sharifimehr, N. Phan, and N. Shamsaei, *Multiaxial fatigue behavior of wrought and additive manufactured Ti-6Al-4V including surface finish effect*. International Journal of Fatigue, 2017. **100**: p. 347-366.
38. Fatemi, A., R. Molaei, S. Sharifimehr, N. Shamsaei, and N. Phan, *Torsional fatigue behavior of wrought and additive manufactured Ti-6Al-4V by powder bed fusion including surface finish effect*. International Journal of Fatigue, 2017. **99**: p. 187-201.
39. Günther, J., D. Krewerth, T. Lippmann, S. Leuders, T. Tröster, A. Weidner, H. Biermann, and T. Niendorf, *Fatigue life of additively manufactured Ti-6Al-4V in the very high cycle fatigue regime*. International Journal of Fatigue, 2017. **94**: p. 236-245.
40. Levy, D., A. Shirizly, and D. Rittel, *Static and dynamic comprehensive response of additively manufactured discrete patterns of Ti6Al4V*. International Journal of Impact Engineering, 2018. **122**: p. 182-196.
41. Mazur, M., M. Leary, M. McMillan, S. Sun, D. Shidid, and M. Brandt, *Mechanical properties of Ti6Al4V and AlSi12Mg lattice structures manufactured by Selective Laser Melting (SLM)*, in *Laser Additive Manufacturing*. 2017. p. 119-161.
42. Pegues, J., M. Roach, R. Scott Williamson, and N. Shamsaei, *Surface roughness effects on the fatigue strength of additively manufactured Ti-6Al-4V*. International Journal of Fatigue, 2018. **116**: p. 543-552.
43. Torres, Y., P. Sarria, F.J. Gotor, E. Gutiérrez, E. Peon, A.M. Beltrán, and J.E. González, *Surface modification of Ti-6Al-4V alloys manufactured by selective laser melting: Microstructural and tribo-mechanical characterization*. Surface and Coatings Technology, 2018. **348**: p. 31-40.
44. Xiao, L. and W. Song, *Additively-manufactured functionally graded Ti-6Al-4V lattice structures with high strength under static and dynamic loading: Experiments*. International Journal of Impact Engineering, 2018. **111**: p. 255-272.

45. Bobbio, L.D., S. Qin, A. Dunbar, P. Michaleris, and A.M. Beese, *Characterization of the strength of support structures used in powder bed fusion additive manufacturing of Ti-6Al-4V*. Additive Manufacturing, 2017. **14**: p. 60-68.
46. Molaei, R., A. Fatemi, and N. Phan, *Significance of hot isostatic pressing (HIP) on multiaxial deformation and fatigue behaviors of additive manufactured Ti-6Al-4V including build orientation and surface roughness effects*. International Journal of Fatigue, 2018. **117**: p. 352-370.
47. Elahinia, M., N. Shayesteh Moghaddam, M. Taheri Andani, A. Amerinatanzi, B.A. Bimber, and R.F. Hamilton, *Fabrication of NiTi through additive manufacturing: A review*. Progress in Materials Science, 2016. **83**: p. 630-663.
48. Mahmoudi, M., G. Tapia, B. Franco, J. Ma, R. Arroyave, I. Karaman, and A. Elwany, *On the printability and transformation behavior of nickel-titanium shape memory alloys fabricated using laser powder-bed fusion additive manufacturing*. Journal of Manufacturing Processes, 2018. **35**: p. 672-680.
49. Shayesteh Moghaddam, N., S.E. Saghayan, A. Amerinatanzi, H. Ibrahim, P. Li, G.P. Toker, H.E. Karaca, and M. Elahinia, *Anisotropic tensile and actuation properties of NiTi fabricated with selective laser melting*. Materials Science and Engineering: A, 2018. **724**: p. 220-230.
50. Zhou, Q., M.D. Hayat, G. Chen, S. Cai, X. Qu, H. Tang, and P. Cao, *Selective electron beam melting of NiTi: Microstructure, phase transformation and mechanical properties*. Materials Science and Engineering: A, 2019. **744**: p. 290-298.
51. Heiden, M.J., L.A. Deibler, J.M. Rodelas, J.R. Koepke, D.J. Tung, D.J. Saiz, and B.H. Jared, *Evolution of 316L stainless steel feedstock due to laser powder bed fusion process*. Additive Manufacturing, 2019. **25**: p. 84-103.
52. Choo, H., K.-L. Sham, J. Bohling, A. Ngo, X. Xiao, Y. Ren, P.J. Depond, M.J. Matthews, and E. Garlea, *Effect of laser power on defect, texture, and microstructure of a laser powder bed fusion processed 316L stainless steel*. Materials & Design, 2019. **164**.
53. Irrinki, H., J.S.D. Jangam, S. Pasebani, S. Badwe, J. Stitzel, K. Kate, O. Gulsoy, and S.V. Atre, *Effects of particle characteristics on the microstructure and mechanical properties of 17-4 PH stainless steel fabricated by laser-powder bed fusion*. Powder Technology, 2018. **331**: p. 192-203.
54. Nath, S.D., H. Irrinki, G. Gupta, M. Kearns, O. Gulsoy, and S. Atre, *Microstructure-property relationships of 420 stainless steel fabricated by laser-powder bed fusion*. Powder Technology, 2019. **343**: p. 738-746.
55. Segura, I.A., L.E. Murr, C.A. Terrazas, D. Bermudez, J. Mireles, V.S.V. Injeti, K. Li, B. Yu, R.D.K. Misra, and R.B. Wicker, *Grain boundary and microstructure engineering of Inconel 690 cladding on stainless-steel 316L using electron-beam powder bed fusion additive manufacturing*. Journal of Materials Science & Technology, 2019. **35**(2): p. 351-367.
56. Wang, X., J.A. Muñoz-Lerma, O. Sánchez-Mata, M. Attarian Shandiz, and M. Brochu, *Microstructure and mechanical properties of stainless steel 316L vertical struts manufactured by laser powder bed fusion process*. Materials Science and Engineering: A, 2018. **736**: p. 27-40.
57. Arisoy, Y.M., L.E. Criales, and T. Özel, *Modeling and simulation of thermal field and solidification in laser powder bed fusion of nickel alloy IN625*. Optics & Laser Technology, 2019. **109**: p. 278-292.
58. Davies, S.J., S.P. Jeffs, M.P. Coleman, and R.J. Lancaster, *Effects of heat treatment on microstructure and creep properties of a laser powder bed fused nickel superalloy*. Materials & Design, 2018. **159**: p. 39-46.
59. Esmailizadeh, R., U. Ali, A. Keshavarzkermani, Y. Mahmoodkhani, E. Marzbanrad, and E. Toyserkani, *On the effect of spatter particles distribution on the quality of Hastelloy X parts made by laser powder-bed fusion additive manufacturing*. Journal of Manufacturing Processes, 2019. **37**: p. 11-20.
60. Zhao, X., J. Chen, X. Lin, and W. Huang, *Study on microstructure and mechanical properties of laser rapid forming Inconel 718*. Materials Science and Engineering: A, 2008. **478**(1-2): p. 119-124.
61. Zhang, D., W. Niu, X. Cao, and Z. Liu, *Effect of standard heat treatment on the microstructure and mechanical properties of selective laser melting manufactured Inconel 718 superalloy*. Materials Science and Engineering: A, 2015. **644**: p. 32-40.
62. Zhang, D., Z. Feng, C. Wang, W. Wang, Z. Liu, and W. Niu, *Comparison of microstructures and mechanical properties of Inconel 718 alloy processed by selective laser melting and casting*. Materials Science and Engineering: A, 2018. **724**: p. 357-367.
63. Yoo, Y.S.J., T.A. Book, M.D. Sangid, and J. Kacher, *Identifying strain localization and dislocation processes in fatigued Inconel 718 manufactured from selective laser melting*. Materials Science and Engineering: A, 2018. **724**: p. 444-451.
64. Xu, Z., J.W. Murray, C.J. Hyde, and A.T. Clare, *Effect of post processing on the creep performance of laser powder bed fused Inconel 718*. Additive Manufacturing, 2018. **24**: p. 486-497.
65. Xu, Z., C.J. Hyde, C. Tuck, and A.T. Clare, *Creep behaviour of inconel 718 processed by laser powder bed fusion*. Journal of Materials Processing Technology, 2018. **256**: p. 13-24.

66. Wang, Z., K. Guan, M. Gao, X. Li, X. Chen, and X. Zeng, *The microstructure and mechanical properties of deposited-IN718 by selective laser melting*. Journal of Alloys and Compounds, 2012. **513**: p. 518-523.
67. Tillmann, W., C. Schaak, J. Nellesen, M. Schaper, M.E. Aydinöz, and K.P. Hoyer, *Hot isostatic pressing of IN718 components manufactured by selective laser melting*. Additive Manufacturing, 2017. **13**: p. 93-102.
68. Tao, P., H. Li, B. Huang, Q. Hu, S. Gong, and Q. Xu, *The crystal growth, intercellular spacing and microsegregation of selective laser melted Inconel 718 superalloy*. Vacuum, 2019. **159**: p. 382-390.
69. Sun, S.-H., Y. Koizumi, T. Saito, K. Yamanaka, Y.-P. Li, Y. Cui, and A. Chiba, *Electron beam additive manufacturing of Inconel 718 alloy rods: Impact of build direction on microstructure and high-temperature tensile properties*. Additive Manufacturing, 2018. **23**: p. 457-470.
70. Sui, S., H. Tan, J. Chen, C. Zhong, Z. Li, W. Fan, A. Gasser, and W. Huang, *The influence of Laves phases on the room temperature tensile properties of Inconel 718 fabricated by powder feeding laser additive manufacturing*. Acta Materialia, 2019. **164**: p. 413-427.
71. Sui, S., J. Chen, E. Fan, H. Yang, X. Lin, and W. Huang, *The influence of Laves phases on the high-cycle fatigue behavior of laser additive manufactured Inconel 718*. Materials Science and Engineering: A, 2017. **695**: p. 6-13.
72. Sheridan, L., O.E. Scott-Emuakpor, T. George, and J.E. Gockel, *Relating porosity to fatigue failure in additively manufactured alloy 718*. Materials Science and Engineering: A, 2018. **727**: p. 170-176.
73. Sangid, M.D., T.A. Book, D. Naragani, J. Rotella, P. Ravi, A. Finch, P. Kenesei, J.-S. Park, H. Sharma, J. Almer, and X. Xiao, *Role of heat treatment and build orientation in the microstructure sensitive deformation characteristics of IN718 produced via SLM additive manufacturing*. Additive Manufacturing, 2018. **22**: p. 479-496.
74. Raza, T., J. Andersson, and L.-E. Svensson, *Microstructure of SLM Alloy 718 in as-manufactured and Post Heat Treated Condition*. 8th Swedish Production Symposium, SPS 2018, 2018.
75. Qi, H., M. Azer, and A. Ritter, *Studies of Standard Heat Treatment Effects on Microstructure and Mechanical Properties of Laser Net Shape Manufactured INCONEL 718*. Metallurgical and Materials Transactions A, 2009. **40**(10): p. 2410-2422.
76. Pröbstle, M., S. Neumeier, J. Hopfenmüller, L.P. Freund, T. Niendorf, D. Schwarze, and M. Göken, *Superior creep strength of a nickel-based superalloy produced by selective laser melting*. Materials Science and Engineering: A, 2016. **674**: p. 299-307.
77. Ni, M., C. Chen, X. Wang, P. Wang, R. Li, X. Zhang, and K. Zhou, *Anisotropic tensile behavior of in situ precipitation strengthened Inconel 718 fabricated by additive manufacturing*. Materials Science and Engineering: A, 2017. **701**: p. 344-351.
78. Ma, D., A.D. Stoica, Z. Wang, and A.M. Beese, *Crystallographic texture in an additively manufactured nickel-base superalloy*. Materials Science and Engineering: A, 2017. **684**: p. 47-53.
79. Kuo, Y.-L., S. Horikawa, and K. Kakehi, *The effect of interdendritic  $\delta$  phase on the mechanical properties of Alloy 718 built up by additive manufacturing*. Materials & Design, 2017. **116**: p. 411-418.
80. Konečná, R., L. Kunz, G. Nicoletto, and A. Bača, *Long fatigue crack growth in Inconel 718 produced by selective laser melting*. International Journal of Fatigue, 2016. **92**: p. 499-506.
81. Juillet, C., A. Oudriss, J. Balmain, X. Feaugas, and F. Pedraza, *Characterization and oxidation resistance of additive manufactured and forged IN718 Ni-based superalloys*. Corrosion Science, 2018. **142**: p. 266-276.
82. Haines, M., A. Plotkowski, C.L. Frederick, E.J. Schwalbach, and S.S. Babu, *A sensitivity analysis of the columnar-to-equiaxed transition for Ni-based superalloys in electron beam additive manufacturing*. Computational Materials Science, 2018. **155**: p. 340-349.
83. Farber, B., K.A. Small, C. Allen, R.J. Causton, A. Nichols, J. Simbolick, and M.L. Taheri, *Correlation of mechanical properties to microstructure in Inconel 718 fabricated by Direct Metal Laser Sintering*. Materials Science and Engineering: A, 2018. **712**: p. 539-547.
84. Deng, D., R.L. Peng, H. Brodin, and J. Moverare, *Microstructure and mechanical properties of Inconel 718 produced by selective laser melting: Sample orientation dependence and effects of post heat treatments*. Materials Science and Engineering: A, 2018. **713**: p. 294-306.
85. Deng, D., J. Moverare, R.L. Peng, and H. Söderberg, *Microstructure and anisotropic mechanical properties of EBM manufactured Inconel 718 and effects of post heat treatments*. Materials Science and Engineering: A, 2017. **693**: p. 151-163.
86. Choi, J.-P., G.-H. Shin, S. Yang, D.-Y. Yang, J.-S. Lee, M. Brochu, and J.-H. Yu, *Densification and microstructural investigation of Inconel 718 parts fabricated by selective laser melting*. Powder Technology, 2017. **310**: p. 60-66.
87. Cakmak, E., M.M. Kirka, T.R. Watkins, R.C. Cooper, K. An, H. Choo, W. Wu, R.R. Dehoff, and S.S. Babu, *Microstructural and micromechanical characterization of IN718 theta shaped specimens built with electron beam melting*. Acta Materialia, 2016. **108**: p. 161-175.

88. Prithivirajan, V. and M.D. Sangid, *The role of defects and critical pore size analysis in the fatigue response of additively manufactured IN718 via crystal plasticity*. *Materials & Design*, 2018. **150**: p. 139-153.
89. Kreitchberg, A., V. Brailovski, and S. Turenne, *Effect of heat treatment and hot isostatic pressing on the microstructure and mechanical properties of Inconel 625 alloy processed by laser powder bed fusion*. *Materials Science and Engineering: A*, 2017. **689**: p. 1-10.
90. Kreitchberg, A., V. Brailovski, and S. Turenne, *Elevated temperature mechanical behavior of IN625 alloy processed by laser powder-bed fusion*. *Materials Science and Engineering: A*, 2017. **700**: p. 540-553.
91. Huynh, L., J. Rotella, and M.D. Sangid, *Fatigue behavior of IN718 microtrusses produced via additive manufacturing*. *Materials & Design*, 2016. **105**: p. 278-289.
92. Chen, Z., S. Chen, Z. Wei, L. Zhang, P. Wei, B. Lu, S. Zhang, and Y. Xiang, *Anisotropy of nickel-based superalloy K418 fabricated by selective laser melting*. *Progress in Natural Science: Materials International*, 2018. **28**(4): p. 496-504.
93. Leary, M., M. Mazur, H. Williams, E. Yang, A. Alghamdi, B. Lozanovski, X. Zhang, D. Shidid, L. Farahbod-Sternahl, G. Witt, I. Kelbassa, P. Choong, M. Qian, and M. Brandt, *Inconel 625 lattice structures manufactured by selective laser melting (SLM): Mechanical properties, deformation and failure modes*. *Materials & Design*, 2018. **157**: p. 179-199.
94. Qin, H., V. Fallah, Q. Dong, M. Brochu, M.R. Daymond, and M. Gallemeault, *Solidification pattern, microstructure and texture development in Laser Powder Bed Fusion (LPBF) of Al10SiMg alloy*. *Materials Characterization*, 2018. **145**: p. 29-38.
95. Uddin, S.Z., L.E. Murr, C.A. Terrazas, P. Morton, D.A. Roberson, and R.B. Wicker, *Processing and characterization of crack-free aluminum 6061 using high-temperature heating in laser powder bed fusion additive manufacturing*. *Additive Manufacturing*, 2018. **22**: p. 405-415.
96. Prasad, K., R. Sarkar, P. Ghosal, and V. Kumar, *Simultaneous creep-fatigue damage accumulation of forged turbine disc of IN 718 superalloy*. *Materials Science and Engineering: A*, 2013. **572**: p. 1-7.
97. Reed, R.C., *The Superalloys: Fundamentals and Applications*, ed. C.U. Press. 2006, Cambridge.
98. Sun, J. and H. Yuan, *Life assessment of multiaxial thermomechanical fatigue of a nickel-based superalloy Inconel 718*. *International Journal of Fatigue*, 2019. **120**: p. 228-240.
99. International, A.W. *Inconel 718*. 2019; Available from: <https://www.alloywire.com/products/inconel-718/>.
100. Akca, E. and A. Gürsel, *A Review on Superalloys and IN718 Nickel-Based INCONEL Superalloy*. *Periodicals of Engineering and Natural Sciences (PEN)*, 2015. **3**(1).
101. Cao, G.H., T.Y. Sun, C.H. Wang, X. Li, M. Liu, Z.X. Zhang, P.F. Hu, A.M. Russell, R. Schneider, D. Gerthsen, Z.J. Zhou, C.P. Li, and G.F. Chen, *Investigations of  $\gamma'$ ,  $\gamma''$  and  $\delta$  precipitates in heat-treated Inconel 718 alloy fabricated by selective laser melting*. *Materials Characterization*, 2018. **136**: p. 398-406.
102. Amato, K.N., S.M. Gaytan, L.E. Murr, E. Martinez, P.W. Shindo, J. Hernandez, S. Collins, and F. Medina, *Microstructures and mechanical behavior of Inconel 718 fabricated by selective laser melting*. *Acta Materialia*, 2012. **60**(5): p. 2229-2239.
103. Mostafa, A., I. Picazo Rubio, V. Brailovski, M. Jahazi, and M. Medraj, *Structure, Texture and Phases in 3D Printed IN718 Alloy Subjected to Homogenization and HIP Treatments*. *Metals*, 2017. **7**(6).
104. Strößner, J., M. Terock, and U. Glatzel, *Mechanical and Microstructural Investigation of Nickel-Based Superalloy IN718 Manufactured by Selective Laser Melting (SLM)*. *Advanced Engineering Materials*, 2015. **17**(8): p. 1099-1105.
105. Tonelli, L., A. Fortunato, and L. Ceschini, *CoCr alloy processed by Selective Laser Melting (SLM): effect of Laser Energy Density on microstructure, surface morphology, and hardness*. *Journal of Manufacturing Processes*, 2020. **52**: p. 106-119.
106. Guo, M., D. Gu, L. Xi, L. Du, H. Zhang, and J. Zhang, *Formation of scanning tracks during Selective Laser Melting (SLM) of pure tungsten powder: Morphology, geometric features and forming mechanisms*. *International Journal of Refractory Metals and Hard Materials*, 2019. **79**: p. 37-46.
107. Khan, H.M., M.H. Dirikolu, E. Koç, and Z.C. Oter, *Numerical investigation of heat current study across different platforms in SLM processed multi-layer AlSi10Mg*. *Optik*, 2018. **170**: p. 82-89.
108. Gribbin, S., S. Ghorbanpour, N.C. Ferreri, J. Bicknell, I. Tsukrov, and M. Knezevic, *Role of grain structure, grain boundaries, crystallographic texture, precipitates, and porosity on fatigue behavior of Inconel 718 at room and elevated temperatures*. *Materials Characterization*, 2019. **149**: p. 184-197.
109. Chlebus, E., K. Gruber, B. Kuźnicka, J. Kurzac, and T. Kurzynowski, *Effect of heat treatment on the microstructure and mechanical properties of Inconel 718 processed by selective laser melting*. *Materials Science and Engineering: A*, 2015. **639**: p. 647-655.
110. Ås, S.K., B. Skallerud, and B.W. Tveiten, *Surface roughness characterization for fatigue life predictions using finite element analysis*. *International Journal of Fatigue*, 2008. **30**(12): p. 2200-2209.

111. Gockel, J., L. Sheridan, B. Koerper, and B. Whip, *The influence of additive manufacturing processing parameters on surface roughness and fatigue life*. International Journal of Fatigue, 2019. **124**: p. 380-388.
112. Balachandramurthi, A.R., J. Moverare, N. Dixit, and R. Pederson, *Influence of defects and as-built surface roughness on fatigue properties of additively manufactured Alloy 718*. Materials Science and Engineering: A, 2018. **735**: p. 463-474.
113. Yadollahi, A., M.J. Mahtabi, A. Khalili, H.R. Doude, and J.C. Newman Jr, *Fatigue life prediction of additively manufactured material: Effects of surface roughness, defect size, and shape*. Fatigue & Fracture of Engineering Materials & Structures, 2018. **41**(7): p. 1602-1614.
114. Kobayashi, K., K. Yamaguchi, M. Hayakawa, and M. Kimura, *Grain size effect on high-temperature fatigue properties of alloy718*. Materials Letters, 2005. **59**(2): p. 383-386.
115. Zhang, Y., L. Yang, T. Chen, W. Zhang, X. Huang, and J. Dai, *Investigation on the optimized heat treatment procedure for laser fabricated IN718 alloy*. Optics & Laser Technology, 2017. **97**: p. 172-179.
116. Anderson, M., A.L. Thielin, F. Bridier, P. Bocher, and J. Savoie,  *$\delta$  Phase precipitation in Inconel 718 and associated mechanical properties*. Materials Science and Engineering: A, 2017. **679**: p. 48-55.
117. Mittra, J., S. Banerjee, R. Tewari, and G.K. Dey, *Fracture behavior of Alloy 625 with different precipitate microstructures*. Materials Science and Engineering: A, 2013. **574**: p. 86-93.
118. Shankar, V., K. Bhanu Sankara Rao, and S.L. Mannan, *Microstructure and mechanical properties of Inconel 625 superalloy*. Journal of Nuclear Materials, 2001. **288**(2): p. 222-232.
119. Mahadevan, S., S. Nalawade, J.B. Singh, A. Verma, B. Paul, and K. Ramaswamy, *Evolution of  $\delta$  phase microstructure in alloy 718*. 7th International Symposium on Superalloy 718 and Derivatives, 2010.
120. Li, J., Z. Zhao, P. Bai, H. Qu, B. Liu, L. Li, L. Wu, R. Guan, H. Liu, and Z. Guo, *Microstructural evolution and mechanical properties of IN718 alloy fabricated by selective laser melting following different heat treatments*. Journal of Alloys and Compounds, 2019. **772**: p. 861-870.
121. Li, S., J. Zhuang, J. Yang, Q. Deng, and J. Du, *The Effect of delta-phase on Crack Propagation Under Creep and Fatigue Conditions in Alloy 718*. Superalloys 718, 625,706 and Various Derivatives, 1994.
122. An, J., L. Wang, Y. Liu, W. Cai, and X. Song, *The role of  $\delta$  phase for fatigue crack propagation behavior in a Ni base superalloy at room temperature*. Materials Science and Engineering: A, 2017. **684**: p. 312-317.
123. Gao, Y., D. Zhang, M. Cao, R. Chen, Z. Feng, R. Poprawe, J.H. Schleifenbaum, and S. Ziegler, *Effect of  $\delta$  phase on high temperature mechanical performances of Inconel 718 fabricated with SLM process*. Materials Science and Engineering: A, 2019. **767**: p. 138327.
124. Schirra, Cales, and Hatala, *The effect of laves phase on the mechanical properties of wrought and cast + HIP Inconel 718*. Superalloys 718, 625 and various derivatives, 1991.
125. Chen, Y., Y. Guo, M. Xu, C. Ma, Q. Zhang, L. Wang, J. Yao, and Z. Li, *Study on the element segregation and Laves phase formation in the laser metal deposited IN718 superalloy by flat top laser and gaussian distribution laser*. Materials Science and Engineering: A, 2019. **754**: p. 339-347.
126. RADHAKRISHNA, C. and K. PRASAD RAO, *Formation and control of Laves phase in superalloy 718 welds*. 1997-04. **v. 32**.
127. Li, J., S.L. Shrestha, Y. Long, L. Zhijun, and Z. Xintai, *The formation of eutectic phases and hot cracks in one Ni-Mo-Cr superalloy*. Materials and Design, 2016. **93**: p. 324-333.
128. You, X., Y. Tan, S. Shi, J.M. Yang, Y. Wang, J. Li, and Q. You, *Effect of solution heat treatment on the precipitation behavior and strengthening mechanisms of electron beam smelted Inconel 718 superalloy*. Materials Science and Engineering A, 2017. **689**: p. 257-268.
129. Tucho, W.M., P. Cuvillier, A. Sjolyst-Kverneland, and V. Hansen, *Microstructure and hardness studies of Inconel 718 manufactured by selective laser melting before and after solution heat treatment*. Materials Science and Engineering: A, 2017. **689**: p. 220-232.
130. Wang, X. and K. Chou, *Effects of thermal cycles on the microstructure evolution of Inconel 718 during selective laser melting process*. Additive Manufacturing, 2017. **18**: p. 1-14.
131. Liu, F., F. Lyu, F. Liu, X. Lin, and C. Huang, *Laves phase control of inconel 718 superalloy fabricated by laser direct energy deposition via  $\delta$  aging and solution treatment*. Journal of Materials Research and Technology, 2020. **9**(5): p. 9753-9765.
132. Xie, H., K. Yang, F. Li, C. Sun, and Z. Yu, *Investigation on the Laves phase formation during laser cladding of IN718 alloy by CA-FE*. Journal of Manufacturing Processes, 2020. **52**: p. 132-144.
133. Huang, W., J. Yang, H. Yang, G. Jing, Z. Wang, and X. Zeng, *Heat treatment of Inconel 718 produced by selective laser melting: Microstructure and mechanical properties*. Materials Science and Engineering: A, 2019. **750**: p. 98-107.
134. Gallmeyer, T.G., S. Moorthy, B.B. Kappes, M.J. Mills, B. Amin-Ahmadi, and A.P. Stebner, *Knowledge of process-structure-property relationships to engineer better heat treatments for laser powder bed fusion additive manufactured Inconel 718*. Additive Manufacturing, 2020. **31**: p. 100977.

135. International, A., *Standard Test Methods for Tension Testing of Metallic Materials*, in *E8/E8M - 15a*. USA.
136. Ahmad, B., S.O. van der Veen, M.E. Fitzpatrick, and H. Guo, *Residual stress evaluation in selective-laser-melting additively manufactured titanium (Ti-6Al-4V) and inconel 718 using the contour method and numerical simulation*. Additive Manufacturing, 2018. **22**: p. 571-582.
137. Konecna, R., G. Nicoletto, L. Kunz, and A. Baca, *Microstructure and directional fatigue behavior of Inconel 718 produced by selective laser melting*. 2016.
138. Moussaoui, Rubio, Mousseigne, Sultan, and Rezai, *Effects of Selective Laser Melting additive manufacturing parameters of Inconel 718 on porosity, microstructure and mechanical properties*. Materials Science and Engineering: A, 2018.
139. Kok, Y., X.P. Tan, P. Wang, M.L.S. Nai, N.H. Loh, E. Liu, and S.B. Tor, *Anisotropy and heterogeneity of microstructure and mechanical properties in metal additive manufacturing: A critical review*. Materials & Design, 2018. **139**: p. 565-586.
140. AlMangour, B. and J.-M. Yang, *Improving the surface quality and mechanical properties by shot-peening of 17-4 stainless steel fabricated by additive manufacturing*. Materials & Design, 2016. **110**: p. 914-924.
141. Zhuang, L. Q. D. R. Sharp, and Paradowska, *Deep surface rolling for fatigue life enhancement of laser clad aluminium alloy*. Applied Surface Science, 2014.
142. Luo, S., W. He, K. Chen, X. Nie, L. Zhou, and Y. Li, *Regain the fatigue strength of laser additive manufactured Ti alloy via laser shock peening*. Journal of Alloys and Compounds, 2018. **750**: p. 626-635.
143. Clauer, A. and J. Koucky, *Laser Shock Processing Increases the Fatigue Life of Metal Parts*. Materials and Processing Report, 1991. **6**(6): p. 3-5.
144. Sundar, Ganesh, R.K. Gupta, Ragvendra, Pant, V. Kain, Ranganathan, R. Kaul, and Bindra, *Laser Shock Peening and its Applications: A Review*. Lasers in Manufacturing and Materials Processing, 2019. **6**(4): p. 424-463.
145. Zhang, Y., J. You, J. Lu, C. Cui, Y. Jiang, and X. Ren, *Effects of laser shock processing on stress corrosion cracking susceptibility of AZ31B magnesium alloy*. Surface and Coatings Technology, 2010. **204**(24): p. 3947-3953.
146. Lu, J.Z., K.Y. Luo, Y.K. Zhang, G.F. Sun, Y.Y. Gu, J.Z. Zhou, X.D. Ren, X.C. Zhang, L.F. Zhang, K.M. Chen, C.Y. Cui, Y.F. Jiang, A.X. Feng, and L. Zhang, *Grain refinement mechanism of multiple laser shock processing impacts on ANSI 304 stainless steel*. Acta Materialia, 2010. **58**(16): p. 5354-5362.
147. Altenberger, I., E.A. Stach, G. Liu, R.K. Nalla, and R.O. Ritchie, *An in situ transmission electron microscope study of the thermal stability of near-surface microstructures induced by deep rolling and laser-shock peening*. Scripta Materialia, 2003. **48**(12): p. 1593-1598.
148. Altenberger, I., R.K. Nalla, Y. Sano, L. Wagner, and R.O. Ritchie, *On the effect of deep-rolling and laser-peening on the stress-controlled low- and high-cycle fatigue behavior of Ti-6Al-4V at elevated temperatures up to 550°C*. International Journal of Fatigue, 2012. **44**: p. 292-302.
149. Dhakal, B. and S. Swaroop, *Effect of laser shock peening on mechanical and microstructural aspects of 6061-T6 aluminum alloy*. Journal of Materials Processing Technology, 2020. **282**.
150. Prevey, Hornbach, and Mason, *Thermal residual stress relaxation and distortion in surface enhanced gas turbine components*. Proceedings of the 17th Heat Treating Society Conference and 1st International Induction Heat Treating Symposium, , 1998.
151. Prevey, *The effect of cold work on the thermal stability of residual compression in surface enhanced IN718*. 20th ASM heat treating society conference proceedings, 2000.
152. Kattoura, M., S.R. Mannava, D. Qian, and V.K. Vasudevan, *Effect of laser shock peening on elevated temperature residual stress, microstructure and fatigue behavior of ATI 718Plus alloy*. International Journal of Fatigue, 2017. **104**: p. 366-378.
153. Navin Kumar, N., A. Chandrakant Yadav, K. Raja, C.D. Naiju, S. Prabhakaran, and S. Kalainathan, *Laser Shock Peening on Al-Si10-Mg Produced by DMLS Technique*. Materials Today: Proceedings, 2020. **22**: p. 2916-2925.
154. Kalentics, N., M.O.V. de Seijas, S. Griffiths, C. Leinenbach, and R.E. Logé, *3D laser shock peening – A new method for improving fatigue properties of selective laser melted parts*. Additive Manufacturing, 2020. **33**.
155. Kalentics, N., E. Boillat, P. Peyre, S. Ćirić-Kostić, N. Bogojević, and R.E. Logé, *Tailoring residual stress profile of Selective Laser Melted parts by Laser Shock Peening*. Additive Manufacturing, 2017. **16**: p. 90-97.